Modulated and Disordered Phases in the System $LiCdVO_4-LiCd_4(VO_4)_3$†

E. Gaudin,*,‡ H. Ben Yahia,‡ F. J. Zúñiga,§ J. M. Pérez-Mato,§ and J. Darriet‡

Institut de Chimie de la Matière Condensée de Bordeaux (ICMCB−CNRS) U.P.R. 9048, Université Bordeaux 1, 87, Av Dr. Schweitzer, 33608 Pessac Cedex, France, and Departamento de Física de la Materia Condensada, Facultad de Ciencia y Tecnología, Universidad del Pais Vasco, Apdo 644, 48080 Bilbao, Spain

Received January 17, 2005. Revised Manuscript Received March 8, 2005

A solid solution $(1-x)LiCdVO_4 - xLi_{1/3}Cd_{1/3}\square_{1/3}CdVO_4$ has been observed for $0 \le x \le 1$. From the cell parameters evolution, two domains of the solid solution have been distinguished with a discontinuity at $x \approx 0.6$. The first one for $0 \le x \le 0.6$ corresponds to the $LiCdVO_4$ substructure of the Na_2CrO_4-type. For $0.75 \le x \le 1$ satellite peaks are observed which correspond to a modulated structure. The first end-member $LiCdVO_4$ ($x = 0$) crystallizes in *Cmcm* space group with $a = 5.911$, $b = 8.975$, and $c = 6.513$ Å. The structure consists of infinite edge-sharing chains of $[CdO_6]$ octahedra linked together by $[VO_4]$ tetrahedra and $[LiO_4]$ tetrahedra. According to the general formula $Li_{1-2x/3}Cd_{x/3}\square_{x/3}CdVO_4$ of the solid solution, when x increases cadmium replaces lithium in the $[LiO_4]$ tetrahedra leading to $[(Li/Cd/\square)O_4]$ disordered tetrahedra. All the phases in the domain $0.7 \le x \le 1$ are one-dimensionally modulated with wavevector $\mathbf{q} = \gamma\mathbf{c}^*$ and γ values of 0.75, 0.733, and 0.722 for $x = {}^3/_4$, ${}^6/_7$, and ${}^9/_{10}$, respectively. The superspace group is $Xmcm(00\gamma)$ where X stands for $({}^1/_2, {}^1/_2, 0, {}^1/_2)$ centering. The main structural result is a strong occupation modulation of lithium and cadmium in the tetrahedral site.

1. Introduction

The polyanionic compounds containing tetrahedral structural units $(XO_4)^{n-}$ (X = P, S, As, Mo, or W), especially the olivine-type compounds, have recently received great attention as candidates for positive electrodes for rechargeable Li-based cells.[1−2] The main limitation for the use of these compounds is their low electronic conductivity. This problem has to be overcome, and recent studies show how it is possible to significantly increase the electronic conductivity of $LiFePO_4$, the most-studied olivine-type compound.[3−4] $LiFePO_4$ has a high lithium intercalation voltage (~3.5 V relative to lithium metal) and high theoretical capacity (170 $mAh{\cdot}g^{-1}$). Among the polyanionic compounds, the $LiMVO_4$ or MVO_4 vanadates series (M = Mn, Fe, Co, Ni, Zn, Cd, In) show different electrochemical properties. They have large reversible capacity for lithium intercalation at low voltage and have been tested as new negative electrode materials.[5−6] According to Denis et al.[6] the most interesting compounds are $InVO_4$ and $FeVO_4$ since they display reversible capacities as large as 900 mAh/g. The vanadates and the phosphates do not crystallize with the same structures and these structural differences can contribute to their different electrochemical behavior.

All the compounds with the general formula $LiM^{+II}PO_4$ when M is a first row transition metal (M = Mn, Fe, Co, Ni) crystallize with the olivine-type structure. In the case of the homologous $LiMVO_4$ compounds, $LiCoVO_4$ and $LiNiVO_4$ crystallize with the spinel-type structure and $LiMnVO_4$ crystallizes with the Na_2CrO_4-type structure. In the case of iron lithium vanadate the existence of iron in its +II oxidation state has not been found in the literature. The synthesis of highly disordered spinel-type compounds $[Li, Fe^{+III}, V^{+III}]_3O_4$ has been reported.[7]

The ideal oxygen packing array in $LiMnPO_4$ (olivine-type structure) and $LiMnVO_4$ (Na_2CrO_4-type structure) compounds are hexagonal and cubic close packing, respectively.[8] In the former structure the lithium atoms occupy the octahedral sites, which form isolated chains by edge sharing. These chains are connected together by $[PO_4]$ tetrahedra and sheets of corner-shared manganese octahedra (Figure 1a). In the $LiMnVO_4$ structure, contrary to the homologous phosphate compound, manganese atoms instead of lithium atoms now fill the edge-sharing chains of octahedra. These chains are linked together by $[VO_4]$ tetrahedra and $[LiO_4]$ tetrahedra (Figure 1b), with the manganese atom being in its +2 oxidation state in both structures.

* To whom correspondence should be addressed. E-mail: gaudin@icmcb-bordeaux.cnrs.fr.

† Part of these results were presented at the 22nd European Crystallography Meeting, Budapest, Hungary, August 26, 2004. An abstract is available in *Acta Crystallogr.* **2004**, *A60*, s187.

‡ Institut de Chimie de la Matière Condensée de Bordeaux.

§ Universidad del Pais Vasco.

(1) Pahdi, A. K.; Nanjundaswamy, K. S.; Goodenough, J. B. *J. Electrochem. Soc.* **1997**, *144*, 1188.
(2) Tarascon, J. M.; Armand, M. *Nature* **2001**, *414*, 359.
(3) Chung, S.-Y.; Bloking, J. T.; Chiang, Y.-M. *Nat. Mater.* **2002**, *1*, 123.
(4) Herle, P. S.; Ellis, B.; Coombs, N.; Nazar, L. F. *Nat. Mater.* **2004**, *3*, 147.
(5) Guyomard, D.; Sigala, C.; Le Gal La Salle, A.; Piffard, J. *J. Power Sources* **1997**, *68*, 692.
(6) Denis, S.; Baudrin, E.; Touboul, M.; Taracon, J.−M. *J. Electrochem. Soc.* **1997**, *144* (12), 4099.
(7) Lenglet, M.; Lensen, M. *Bull. Soc. Chim. Fr.* **1964**, *1964*, 26.
(8) Gaudin, E.; Ben Yahia, H.; Shikano, M.; zur Loye, H. C.; Darriet, J. *Z. Kristallogr.* **2004**, *219*, 755.

10.1021/cm050104e CCC: $30.25
Published on Web 04/08/2005

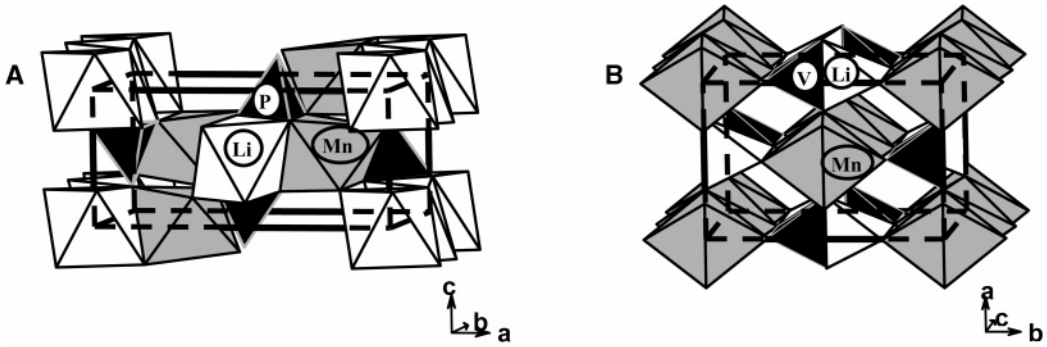

Figure 1. View of the (A) $LiMnPO_4$ and (B) $LiMnVO_4$ structures.

Recently we have determined the crystal structure of the incommensurate modulated compound $LiCd_4(VO_4)_3$ which crystallizes with the Na_2CrO_4 structure.[8] The modulation of the structure was mainly due to the cationic ordering between lithium and cadmium atoms in one tetrahedral site. The overall formula can be expressed as $Li_{1/3}Cd_{1/3}\square_{1/3}CdVO_4$ by analogy with $LiCdVO_4$ where two-thirds of Li^+ ion in one tetrahedral site are replaced by only one-third of Cd^{2+} to keep the charge balance and therefore cationic vacancies $\square$ are created. The aim of this work is the structural study of the system $(1-x)LiCdVO_4 - xLi_{1/3}Cd_{1/3}\square_{1/3}CdVO_4$ ($0 \le x \le 1$) where different modulated structures related to the x value can be observed. The general formula of the system can be expressed as $Li_{1-2x/3}Cd_{x/3}\square_{x/3}CdVO_4$ with the two limits $x = 0$ corresponding to $LiCdVO_4$ and $x = 1$ to $LiCd_4(VO_4)_3$. For $0.75 \le x \le 1$, incommensurate modulated structures have been observed and a close dependence of the wavevector with the x value has been evidenced and described by a unique structural model.

2. Experimental Section

2.1. Synthesis and Crystallization. Powder samples of $LiCdVO_4$ and $LiCd_4(VO_4)_3$ were prepared by the direct solid-state reaction of stoichiometric amounts of the starting reagents CdO (prepared by the thermal decomposition of $CdCO_3$ at 500 °C), Li_2CO_3, and V_2O_5. The mixtures were ground in an agate mortar and heated at 700 °C for 12 h in gold crucibles under an oxygen atmosphere. This procedure was repeated three times to ensure complete reaction and formation of a single phase product. All the compounds with composition $Li_{1-2x/3}Cd_{x/3}CdVO_4$ ($0 < x < 1$) have been prepared from the stoichiometric mixture of the two end-members $LiCdVO_4$ and $LiCd_4(VO_4)_3$. The mixtures were heated at 700 °C in gold crucibles for 4 days with intermediate grinding.

Single crystals of $Li_{1-2x/3}Cd_{x/3}CdVO_4$ ($x = 0$, $^1/_3$, $^3/_4$, $^6/_7$, $^9/_{10}$) were prepared by melting the powder samples of the corresponding phases at 950 °C followed by slow cooling at 5 °C/hours down to room temperature. Part of the crystals obtained after crystallization were ground and measured on the X-ray powder diffractometer. After each crystallization a single phase was observed with crystallographic data similar to those obtained from the powder sample study. This allowed us to confirm the nominal composition of the single crystals. The selection of high-quality single crystals was based upon the size and the sharpness of the diffraction spots.

2.2. X-ray Powder Diffraction Study. X-ray powder diffraction data of all the products were collected at room temperature over the angular range $5° \le 2\theta \le 120°$ with a step size of $\Delta(2\theta) = (0.02)°$ using a Philips X-pert diffractometer operating with Cu Kα radiation.

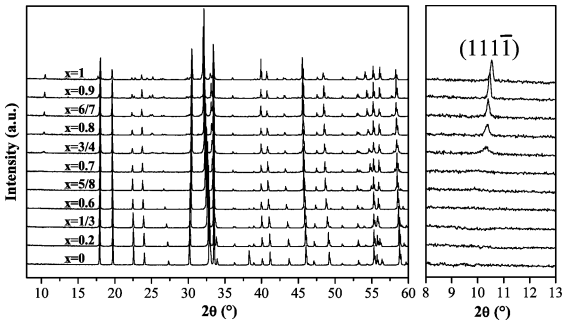

Figure 2. X-ray powder diffractograms of the series of compounds $Li_{1-2x/3}Cd_{x/3}CdVO_4$ with $0 \le x \le 1$. In the right part the evolution of satellite reflections $(111\bar{1})$ is emphasized.

The X-ray diffraction data were refined by a Le Bail profile analysis[9] using the Jana2000 program package.[10] The background was estimated by a Legendre polynom and the peak shapes were described by a pseudo-Voigt function varying five profile coefficients.[11] The refinement of peaks asymmetry was performed using four parameters.[12] When satellite peaks are observed all the peaks have been indexed by four integers *hklm* and the reflections conditions were compatible with the space group $Cmcm(10\gamma)$ with $\mathbf{q} = 1\mathbf{a^*} + \gamma\mathbf{c^*}$ or the equivalent space group $Xmcm(00\gamma)$ with $\mathbf{q} = \gamma\mathbf{c^*}$ where X stands for ($^1/_2$, $^1/_2$, 0, $^1/_2$) centring (see next section and ref 8). For $x < 0.75$ the *Cmcm* conventional space group extinction conditions have been used for the Le Bail refinement.

Figure 2 shows the evolution of the X-ray diffraction patterns of the $Li_{1-2x/3}Cd_{x/3}\square_{x/3}CdVO_4$ system for $0 \le x \le 1$. A structural change is clearly observed for $x = {}^3/_4$ with the appearance of satellite peaks as it has been previously observed for $Li_{1/3}Cd_{1/3}CdVO_4$.[8] The satellite peaks intensity grows with further increase in cadmium content as emphasized in the right part of Figure 2. A decrease of the satellite peaks width is also observed and this can be correlated to a decrease of the cationic disorder in the tetrahedral site when cadmium content increases (vide infra).

Figure 3 shows the evolution of the unit cell parameters with x value for $Li_{1-2x/3}Cd_{x/3}CdVO_4$. A complete solid solution exists between the two end-members $LiCdVO_4$ and $Li_{1/3}Cd_{1/3}CdVO_4$. Two distinct regions are observed with a linear evolution of the cell parameters and volume for both regions, a discontinuity appearing between the compositions $x = 0.6$ and $x = 0.625$. In both regions the a parameter decreases while the b and c parameters increase.

(9) Le Bail, A.; Duroy, H.; Fourquet, J. L. *Mater. Res. Bull.* **1988**, *23*, 447.
(10) Petricek, V.; Dusek, M. *The crystallographic computing system Jana 2000*; Institute of Physics: Praha, Czech Republic, 2000.
(11) Thompson, P.; Cox, D. E.; Hastings, J. B. *J. Appl. Crystallogr.* **1987**, *20*, 79.
(12) Berar, J. F.; Baldinozzi, G. *J. Appl. Crystallogr.* **1993**, *26*, 128.

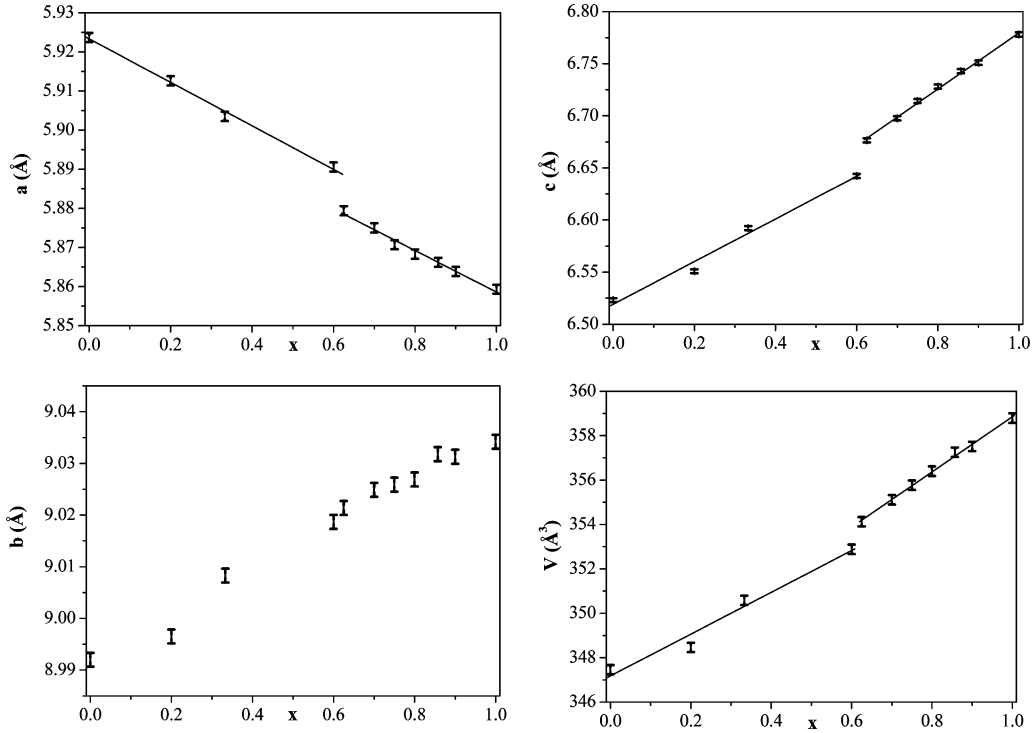

Figure 3. Evolution of the unit cell parameters with the composition x for $Li_{1-2x/3}Cd_{x/3}CdVO_4$.

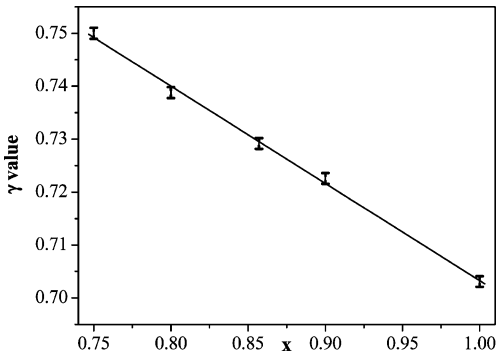

Figure 4. Evolution of the component of the **q**-vector (**q*** = **c***) for $0.75 \leq x \leq 1$.

The main variation is observed for c parameter with a relative increase of 3.3% between $LiCdVO_4$ and $Li_{1/3}Cd_{1/3}CdVO_4$. This observation is in agreement with the structure of $Li_{1/3}Cd_{1/3}CdVO_4$ where the shift of the cadmium position in the tetrahedra $[Li_{1-2x/3}Cd_{x/3}\square_{x/3}]O_4$ induces an elongation of the tetrahedra edge parallel to the **c** axis (see discussion in next section).

For compositions between the discontinuity ($x \approx 0.6$) and $x = 0.7$ satellite peaks are not observed but probably due to small amplitudes of the modulation given place to very weak satellite peaks. The evolution of the γ component of the **q**-vector for $0.75 \leq x \leq 1$ is displayed in Figure 4. One can notice that this variation is linear with the x value and for $x = 0.75$ the γ value is equal to $^3/_4$ and corresponds to a commensurate case. The structural study of crystals with composition ranging between $0.75 \leq x \leq 1$ will help to understand this evolution.

2.3. Single Crystal. Single-crystal X-ray diffraction data from samples with composition $x = 0$, $^1/_3$, $^3/_4$, $^6/_7$, and $^9/_{10}$ were collected on image plate and CCD-detector diffractometers with sealed-tube Mo Kα X-ray sources. Details about the five different experiments are summarized in Tables 1 and 2. Data reduction applied to the different data sets was performed using the specific programs of the diffractometers, and program package Jana2000[10] was used for the numerical absorption correction and structure refinements.

Table 1. Crystallographic Data and Structure Refinement for $LiCdVO_4$ and $Li_{7/9}Cd_{1/9}CdVO_4$

formula	$LiCdVO_4$	$Li_{7/9}Cd_{1/9}CdVO_4$
crystal color	orange	
mol wt (g mol^{-1})	234.29	245.23
cryst syst	orthorhombic	
space group	*Cmcm*	
parameters	5.9112(4) Å	5.9006(5) Å
	8.9750(5) Å	9.0001(6) Å
	6.5135(5) Å	6.5877(3) Å
V (Å^3)	345.56(2)	349.85(4)
Z	4	4
D_x (g·cm^{-3})	4.502	4.654
cryst shape	lamellar	
cryst size (mm)	0.110 × 0.050 × 0.014	0.132 × 0.121 × 0.03
temperature (K)	293	
diffractometer	Enraf-Nonius KappaCCD	
monochromator	oriented graphite	
radiation	Mo Kα ($\lambda = 0.71069$ Å)	
scan mode	Phi-scan + ω-scan	Phi-scan + ω-scan
no. images	372	332
$h\,k\,l$ range	$-10 < h < 10$	$-10 < h < 10$
	$-14 < k < 16$	$-14 < k < 16$
	$-11 < l < 11$	$-11 < l < 11$
θ_{max}	40°	
abs coeff (mm^{-1})	8.70	9.25
abs correction	Gaussian	
T_{min}/T_{max}	0.521/0.889	0.346/0.736
no. of reflns	5239	4944
R_{int}	0.0447	0.0449
no. ind reflns	607	615
reflns with $I > 2\sigma(I)$	555	586
refinement	F^2	
F(000)	424	443
R factors	R(F) = 0.0183	R(F) = 0.0144
	wR(F^2) = 0.0475	wR(F^2) = 0.0423
no. params	28	30
GOF	1.21	1.06
weighting scheme	$w = 1/(\sigma^2(I) + 0.0009I^2)$	
diff. Fourier residues (e$^-$/Å^3)	[−1.03, +0.77]	[−0.79, +0.86]

In the case of $x = ^3/_4$, $^6/_7$, and $^9/_{10}$, precession diffraction patterns simulated from the collected frame images showed strong main reflections and weak satellites reflections. The basic cell defined

Table 2. Crystal Data and Structure Refinement of Modulated Compounds

formula		$(Li_{1-2x/3}Cd_{x/3}\square_{x/3})CdVO_4$	
composition x	9/10	6/7	3/4
crystal color		orange	
mol wt	263.85	262.44	258.93
cryst syst		orthorhombic	
superspace group		$Xmcm(00\gamma)000$ (X: ($^1/_2$ $^1/_2$ 0 $^1/_2$))	
parameters a (Å)	5.8640(5)	5.8676(5)	5.8705(10)
b (Å)	9.0240(10)	9.0327(8)	9.028(2)
c (Å)	6.7515(1)	6.7450(6)	6.7112(6)
V (Å^3)	357.27(6)	357.49(5)	355.68(10)
γ ($\mathbf{q} = \gamma\mathbf{c^*}$)	0.722	0.733	0.75
Z		4	
D_x (g·cm^{-3})	4.904	4.875	4.834
cryst shape		prismatic	
cryst size (mm)	0.141 × 0.103 × 0.084	0.133 × 0.109 × 0.096	0.05 × 0.022 × 0.012
temperature (K)		293	
diffractometer	Stoe IP	Oxford Diff. CCD	Enraf-Nonius CCD
radiation		Mo Kα	
scan mode	Phi-scan	ω-scan	Phi-scan + ω-scan
no. images	200	1697	561
$hklm$ range	$-7 < h < 7$	$-8 < h < 11$	$-9 < h < 9$
	$-11 < k < 11$	$-10 < k < 17$	$-14 < k < 14$
	$-9 < l < 9$	$-13 < l < 13$	$-11 < l < 11$
	$-2 < m < 2$	$-2 < m < 2$	$-2 < m < 2$
θ_{max}(deg)	30	45	35
abs coeff. (mm^{-1})	10.15	10.06	9.90
abs correction		Gaussian	
T_{min}/T_{max}	0.329/0.542	0.304/0.504	0.644/0.897
obs. criterion		$I > 3\sigma(I)$	
no. reflec.(total/obs.)	17258/4862	22577/11141	27370/11525
main (total/obs.)	311/304	804/702	879/743
satellites 1 (total/obs.)	581/505	1516/846	1632/625
satellites 2 (total/obs.)	581/349	1510/720	1418/226
R_{int} (obs.)	0.0533	0.0767	0.0517
F(000)	474	472	466
refinement		F	
R/R_w (obs)	0.0349/0.0480	0.0419/0.0491	0.0375/0.0415
R_o (main_obs)	0.0189/0.0276	0.0305/0.0359	0.0215/0.0276
R_1(sat_1_obs)	0.0303/0.0315	0.0413/0.0390	0.0678/0.0553
R_2(sat_2_obs)	0.1286/0.1145	0.0876/0.0988	0.1891/0.1773
no. params	86	89	87
weighting scheme		$w = 1/(\sigma^2(I) + 0.0001I^2)$	$w = 1/(\sigma^2(I) + 0.000225I^2)$
GOF	2.67	1.45	1.47
diff. Fourier (e/A^3)	[−1.46, 1.93]	[−3.17, 4.09]	[−4.03, 4.44]

from main reflections corresponds to an orthorhombic structure with *Cmcm* space group and lattice parameters given in Table 2. All the superstructure reflections could be interpreted as first and second-order satellites with a unique modulation wavevector $\mathbf{q} = \mathbf{a^*} + \gamma\mathbf{c^*}$ and γ values varying from 0.722 for the composition with $x = {}^9/_{10}$ to 0.75 for $x = {}^3/_4$ (see Table 2). The different values of γ were calculated from the position of satellites using specific software routines included in the diffractometer software packages. The determined values of $\gamma = 0.703$ for $x = 1^8$ and $\gamma = 0.75$ for $x = {}^3/_4$ could be approximated to the rational numbers $^7/_{10}$ and $^3/_4$, respectively.

During the indexing process of the collected data, all the satellites were indexed with four indices ($hklm$) of diffraction vectors $h\mathbf{a^*}+k\mathbf{b^*}+l\mathbf{c^*}+m\mathbf{q}$. According to this indexation the observed systematic absences ($hklm$) $h + k = 2n + 1$ and ($h0lm$) $l = 2n + 1$ are compatible with superspace groups $Cmcm(10\gamma)000$, $Cmc2_1(10\gamma)000$ and $C2cm(10\gamma)000$ (International Tables of Crystallography, vol. C, 2004). However, it is more convenient to eliminate the rational component $1\mathbf{a^*}$ of the $\mathbf{q}$ vector and introduce a superspace centring translation ($^1/_2$, $^1/_2$, 0, $^1/_2$). In this setting the superspace group symbol becomes $Xmcm(00\gamma)000$ (the same change of setting can be done for the noncentrosymmetric groups), with generators (x, y, z, x_4), ($-x$, y, z, x_4), (x, $-y$, $^1/_2 + z$, x_4), ($-x$, $-y$, $^1/_2 + z$, x_4).

3. Refinements

3.1. Structure Determination of Non-modulated Phases $LiCdVO_4$ and $Li_{7/9}Cd_{1/9}\square_{1/9}CdVO_4$ ($x = {}^1/_3$). The structure of $LiCdVO_4$ was solved in the space group *Cmcm*. The atomic positions were deduced from direct method and difference Fourier analysis. With isotropic atomic displacement parameter (ADP), the residual factor converged to R(F) = 0.0363 (wR(F^2) = 0.0931). The use of anisotropic displacement parameter for all positions, and the introduction of an isotropic secondary extinction lowered it to R(F) = 0.0210 (wR(F^2) = 0.0522). At this stage lithium position exhibited nondefinite positive ADP and a residual electron density was found close to the lithium position. As a substitution of the lithium by cadmium is possible the residual density has been attributed to a small amount of cadmium on the lithium site. A mixed model with slightly different y-coordinate for Cd and Li has been used. Lithium substitution has been done on the cadmium site to keep the stoichiometry safe. To avoid strong correlation for the refinement of the occupancy of the two split positions a unique anisotropic displacement tensor was used. With this split model, the residual factor converged to R(F) = 0.0183 (wR(F^2) = 0.0475) and the difference Fourier residues were reduced to a nonsignificant noise (Table 1). The final atomic site parameters are given in Table 3 with interatomic distances given in Table 4. Several crystals of the as-prepared phase $LiCdVO_4$ have been tested and a small disorder in the lithium tetrahedral site has been always observed.

Table 3. Fractional Atomic Coordinates and Equivalent Isotropic Displacement Parameters (Å²) for $LiCdVO_4$ ($x = 0$ first line) and $Li_{7/9}Cd_{1/9}\square_{1/9}CdVO_4$ ($x = 1/3$ s line)

	Wyckoff position		*x*	*y*	*z*	U_{eq}	site occup.
Cd1	4a	0	0	1/2	0.00889(6)	0.965(2)
		0	0	1/2	0.01138(5)	1
Li1	4a	0	0	0.5	0.00889	0.035
V1	4c	0	0.64026(6)	3/4	0.00783(11)	1
		0	0.64093(4)	3/4	0.00968(8)	1
Li2	4c	0	0.343(3)	3/4	0.030(4)	0.965
		0	0.3391(10)	3/4	0.021(2)	0.778
Cd2	4c	0	0.313(4)	3/4	0.030	0.035
		0	0.3032(3)	3/4	0.0235(6)	0.111
O1	8g	0.2315(3)	0.4805(2)	1/4	0.0112(3)	1
		0.2337(2)	0.47833(13)	1/4	0.0129(2)	1
O2	8f	0	0.2551(2)	0.4640(3)	0.0146(4)	1
		0	0.25391(15)	0.4612(2)	0.0195(3)	1

Table 4. Main Interatomic Distances (Å), Bond Valences (BV),[a] and Bond Valence Sums (BVS) for $LiCdVO_4$ ($x = 0$) and $Li_{7/9}Cd_{1/9}\square_{1/9}CdVO_4$ ($x = 1/3$)

	$LiCdVO_4$			$Li_{7/9}Cd_{1/9}CdVO_4$		
	distance	BV	BVS	distance	BV	BVS
Cd1−O1 (×4)	2.2806(12)	0.36		2.2846(8)	0.36	
Cd1−O2 (×2)	2.302(2)	0.34		2.299(2)	0.34	
Cd1			2.13			2.12
V1−O2 (×2)	1.681(2)	1.39		1.6828(15)	1.38	
V1−O1 (×2)	1.746(2)	1.17		1.7473(11)	1.16	
V1			5.12			5.09
Li2−O2 (×2)	2.023(11)	0.22		2.051(4)	0.21	
Li2−O1 (×2)	2.09(2)	0.19		2.146(7)	0.16	
Li2			0.81			0.73
Cd2−O2 (×2)	1.934(10)	0.92		1.9536(15)	0.88	
Cd2−O1 (×2)	2.30(3)	0.34		2.402(2)	0.26	
Cd2−O2 (×2)	3.08(3)	0.04		2.981(3)	0.05	
Cd2			2.61			2.38
V1−Li2	2.67(3)			2.717(9)		
V1−Cd2	2.94(4)			3.040(3)		

[a] $BV = e^{(r_0 - r)/B}$ with the following parameters:[16] $B = 0.37$ Å, $r_0(Cd^{2+}-O^{2-}) = 1.904$ Å, $r_0(V^{5+}-O^{2-}) = 1.803$ Å, $r_0(Li^{+}-O^{2-}) = 1.466$ Å.

The same structural model has been used for the $Li_{7/9}Cd_{1/9}\square_{1/9}CdVO_4$ study with no disorder on the cadmium octahedral site, with the disorder being only considered for the lithium tetrahedral site. The following constraint on lithium tetrahedral site occupancy has been introduced to keep the electroneutrality: $occ(Li) = 1 - 2 \times occ(Cd)$. The residual factor converged to $R(F) = 0.0144$ ($wR(F^2) = 0.04423$) with nonsignificant difference Fourier residues (Table 1).

3.2. Single-Crystal X-ray Diffraction Study of $Li_{1/2}Cd_{1/4}CdVO_4$ ($x = 3/4$), $Li_{3/7}Cd_{2/7}CdVO_4$ ($x = 6/7$), $Li_{4/10}Cd_{3/10}CdVO_4$ ($x = 9/10$), and $Li_{1/3}Cd_{1/3}CdVO_4$ ($x = 1$). *3.2.1 Continuous and Crenel Modulation Models.* The structural refinements of phases $x = 9/10$, $6/7$, and $3/4$ were conducted through similar steps. First, a three-dimensional average structure was refined using main reflections and *Cmcm* space group. This model corresponds to the structure of $LiCdVO_4$ where the Li position is partially replaced by Cd (Cd2) and Li (Li2). The refinement of this model leads to fractional occupation of Cd2 close within standard deviation to the nominal value of the formula. Due to the small electronic charge of Li against the Cd atom, refinement of the occupation parameter of Li2 showed an unstable behavior and was fixed to the exact value according to the formula. Projections of the average structure are shown in Figure 5.

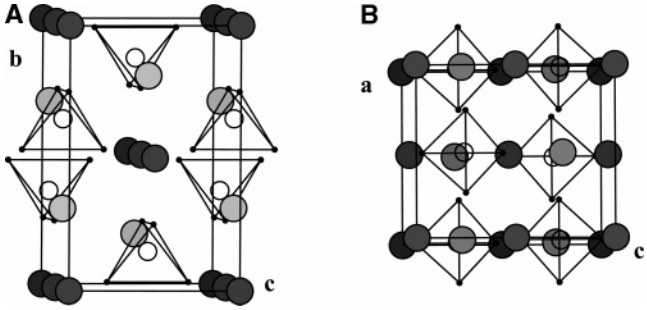

Figure 5. (A) *ac* and (B) *bc* Projections of the average structure. Black spheres represent Cd1 position, medium-gray spheres indicate Cd2/Li2 positions, and small circles are V atoms surrounded by oxygen-tetrahedra.

An incommensurate model based on the centrosymmetric $Xmcm(00\gamma)000$ superspace group was refined, first with continuous occupational modulation for Cd2 and Li2 atoms and displacive harmonic modulations for all atoms. Starting with average basic atomic coordinates, the incommensurate structure was modeled with up to second order Fourier terms in the occupational modulation for Cd2 and first order ones for Li2. Displacive atomic modulation functions (AMF) were added to all atoms in subsequent refinements and, during last refinement steps, anisotropic and modulations of thermal displacements were introduced for all Cd, V, and O atoms. Note that the atoms in special positions have restrictions on the components of their harmonic amplitudes. As an example, the occupancy modulations of Cd2 and Li2 contain only cosinus terms. In the case of $x = 3/4$, second-order satellites $(h,k,l,2)$ and $(h,k,l+3,-2)$ exactly superpose in the diffraction pattern and consequently, the superspace refinement of that phase was performed using in JANA2000 the commensurate option and choosing the section at $t = 1/16$, which gives a three-dimensional structure with the *Im*2*m* space group, compatible with the observed systematic extinctions. In data sets of compounds $x = 9/10$ and $6/7$, the superposition of second-order satellites was checked within 0.5°. Details of the least-squares parameters and reliability R-factors are given in Table 2, the final atomic parameters are summarized in Tables 5−7, and plots of the occupancy functions of Cd2 and Li2 atoms are drawn in Figure 6.

The shape of the occupancy modulation functions suggests that the distribution of the Cd2/Li2 atoms could also be described by using special functions as the crenel functions.[13] The use of these functions allows the presence of discontinuities in the modulation functions and a small number of refinement parameters for highly anharmonic modulations. On the other hand, the introduction of these discontinuous functions in the description of the occupational modulations requires, in general, to change the usual basis of cosinus and sinus functions for describing the displacive modulations to a basis of functions orthogonalized in the occupation interval defined by the crenel functions. This procedure is available in the JANA2000 program[10] and has been tested as an alternative model of the Cd2/Li2 distribution. The model has been also applied to the compound with $x = 1$, using in the refinement the experimental data already published.[8] The crenel function consists of a periodic steplike occupational

(13) Petricek, V.; van der Lee, A.; Evain, M. *Acta Crystallogr., Sect. A: Found. Crystallogr.* **1995**, *51*, 529.

Table 5. Final Atomic Coordinates, Fourier Amplitudes of the Occupancy and Displacive Modulation Functions, and Equivalent Isotropic Thermal Displacements of Compounds with Composition $x = {}^{9}/_{10}$[a]

atom		occ.	x	y	z	U_{eq}
Cd1			0	0	0.5	0.0098(4)
	s,1		0	0.01425(7)	0.00358(4)	
	c,1		0	0	0	
	s,2		0	0.00501(9)	0.00161(9)	
	c,2		0	0	0	
	s,3		0	0.0003(4)	−0.0093(6)	
	c,3		0	0	0	
	s,34		0	0.0048(15)	0.010(2)	
	c,4		0	0	0	
Cd2		0.3	0	0.3115(6)	0.75	0.0309(12)
	s,1	0	0	0	0.0067(2)	
	c,1	0.414(7)	0	−0.0109(7)	0	
	s,2	0				
	c,2	0.098(2)				
Li2		0.4	0	0.321(9)	0.75	0.0804
	s,1	0	0	0	0.0065	
	c,1	−0.2(2)	0	−0.0117	0	
V1			0	0.64205(9)	0.75	0.0050(6)
	s,1		0	0	−0.00180(11)	
	c,1		0	−0.00188(8)	0	
	s,2		0	0	−0.0090(2)	
	c,2		0	−0.00277(13)	0	
	s,3		0	0	−0.0234(14)	
	c,3		0	0.000(3)	0	
O1			0.2600(5)	0.0273(3)	0.75	0.0128(6)
	s,1		0	0	0.0006(3)	
	c,1		−0.0071(4)	0.0128(3)	0	
	s,2		0	0	−0.0028(3)	
	c,2		−0.0035(5)	0.0020(5)	0	
O2			0	0.2505(4)	0.4541(6)	0.0216(7)
	s,1		0	0.0054(3)	−0.0031(4)	
	c,1		0	0.0018(3)	0.0035(4)	
	s,2		0	0.0063(4)	0.0046(5)	
	c,2		0	0.0055(4)	0.0152(4)	

[a] Occupancy modulation is $P = P_o + c_1\cos(2\pi x_4) + c_2\cos(4\pi x_4)$ Displacive modulation is $U = s_n(\sin(2\pi n x_4) + c_n\cos(2\pi n x_4)$.

wave defined by means of two parameters: the step-width Δ and its center x_{o4} along the internal coordinate x_4, with an occupation parameter p inside the step and 0 elsewhere. According to the results of the continuous model, the center of the crenel functions for Cd2 is $x_{o4} = 0$, whereas the width Δ should be determined by the composition formula, having values of ${}^{1}/_{3}$, ${}^{3}/_{10}$, ${}^{2}/_{7}$, and ${}^{1}/_{4}$ for compositions $x = 1$, ${}^{9}/_{10}$, ${}^{6}/_{7}$, and ${}^{3}/_{4}$, respectively. As the occupation functions of Li2 are ${}^{1}/_{2}$ shifted along the internal coordinate x_4, the associated crenel is at $x_{o4} = 0.5$ and the corresponding widths are ${}^{1}/_{3}$, ${}^{3}/_{7}$, ${}^{4}/_{10}$, and ${}^{1}/_{2}$, respectively. Using these parameters to define the crenels and the same number of AMF as used with the continuous-occupancy model for all atoms, the refinements converge to R-factors higher than those obtained in the continuous modulations models. However, letting free the width of the crenels together with the site multiplicity of Cd2 atom, the refinements converge to R-factors as low as in the continuous model refinements. Attempts to refine the crenel-width of Li2 led to unreasonable values of this parameter and it was fixed to the value calculated from the formula assuming a fully occupied crenel. The resulting parameters defining the crenels and R-factors are summarized in Table 8. Although the resulting occupancy p and crenel-width Δ values should fulfill the condition ${}^{x}/_{3} = p\Delta$ giving the total amount of Cd2 in the formula, the two parameters were refined without any restriction. The refined values satisfy, however, this condition fairly well.

A more sophisticated refinement could be imagined combining the crenel model with a modulation of the fractional occupancy. Although such a combination of refining parameters is not allowed in the program, it would be interesting to test such a possibility to see if the crenel-width and occupancy values behavior with composition in a similar way or related to that of the modulation wavevector **q**. Unfortunately, such a combination of refining variables is not (yet) implemented in JANA2000 program.

3.2.2 Commensurate Supercell Model of $x = {}^{3}/_{4}$. The commensurate value of the modulation wavevector in the phase with composition $x = {}^{3}/_{4}$ allows a standard description of the diffraction pattern in terms of a supercell with a lattice constant $c = 4c_o$.

One of the properties of the superspace formalism is that the real-space structure is generated as a section of the corresponding superspace structure.[14] As it was mentioned in Section 3.2.1, the chosen section at $t = {}^{1}/_{16}$ gives a three-dimensional structure with the *Im*2*m* space group. The three-dimensional supercell contains 16 formula units $(Li_{1/2}Cd_{1/4}\square_{1/4})$-$CdVO_4$ giving 8 Li2, 4 Cd2, 16 Cd1, 16 V, and 64 O atoms. The single independent position of Cd2/Li2 atom in the average cell used for the superspace description expands into 5 independent positions in the supercell, two of them with multiplicity 2 and three with multiplicity 4. These positions (16 including the symmetry equivalent) should be shared, in principle, among 8 Li2 and 4 Cd2 atoms, with occupancies in accord with those calculated from the refined occupancy

(14) De Wolf, P. M. *Acta Crystallogr., Sect. A: Found. Crystallogr.* **1974**, *30*, 777.

Table 6. Final Atomic Coordinates, Fourier Amplitudes of the Occupancy and Displacive Modulation Functions, and Equivalent Isotropic Thermal Displacements of Compounds with Composition $x = 6/7$[a]

atom		occ.	x	y	z	U_{eq}
Cd1			0	0	0.5	0.01242(6)
	s,1		0	0.01340(4)	0.00328(3)	
	c,1		0	0	0	
	s,2		0	0.00488(3)	0.00267(4)	
	c,2		0	0	0	
	s,3		0	0.0017(2)	−0.0044(2)	
	c,3		0	0	0	
Cd2		0.2825(15)	0	0.3107(3)	0.75	0.0367(9)
	s,1	0	0	0	0.0048(2)	
	c,1	0.392(4)	0	−0.0103(4)	0	
	s,2	0				
	c,2	0.0765(11)				
Li2		0.4286	0	0.338(2)	0.75	0.001(2)
	s,1	0	0	0	0.009(2)	
	c,1	−0.05(5)	0	0.009(2)	0	
V1			0	0.64225(6)	0.75	0.0068(2)
	s,1		0	0	−0.00134(7)	
	c,1		0	−0.00199(6)	0	
	s,2		0	0	−0.00995(11)	
	c,2		0	−0.00304(7)	0	
	s,3		0	0	−0.0220(4)	
	c,3		0	−0.0008(14)	0	
O1			0.2602(3)	0.0273(2)	0.75	0.0146(3)
	s,1		0	0	0.0005(2)	
	c,1		−0.0066(3)	0.01241(19)	0	
	s,2		0	0	−0.0034(2)	
	c,2		−0.0041(3)	0.0020(2)	0	
O2			0	0.2514(2)	0.4533(3)	0.0240(4)
	s,1		0	0.0052(2)	−0.0036(3)	
	c,1		0	0.0015(2)	0.0030(3)	
	s,2		0	0.0036(2)	0.0026(3)	
	c,2		0	0.0058(2)	0.0178(3)	

[a] Occupancy modulation is $P = P_o + c_1\cos(2\pi x_4) + c_2\cos(4\pi x_4)$ Displacive modulation is $U = s_n(\sin(2\pi n x_4) + c_n\cos(2\pi n x_4)$.

modulation function. The rest of the atoms (Cd1, V, and O) are unambiguously positioned in the supercell. Starting with this model, a few refinement cycles showed that Cd2 is basically distributed among three positions with occupancy fractions of 0.502 (Cd21), 0.464 (Cd22), and 0.286 (Cd23), whereas more doubts arise about the distribution of the Li atoms. As two free-Cd2 positions remain, it was expected that they are fully occupied with Li atoms, this accounting for 6 Li atoms and leaving 2 Li for sharing positions with Cd2. Subsequent refinements testing different distributions for Li do not show significant differences, but in all cases large correlations appear between parameters of atoms sharing the same sites. At this point, one Li atom (Li3) was placed with occupancy 0.5 at the site of the Cd2 atom with lower occupancy. At the end of refinement, an R-factor of 3.81% (wR = 4.03%) was obtained, including anisotropic displacements for all atoms except Li. Final atomic parameters are given in Table 9, where an origin shift with respect to the incommensurate basic unit cell has been introduced in order to use the standard setting of the *Im*2*m* space group.

As it was mentioned above, sections of the superspace model at different t values generate two monoclinic structures, each of them giving different structural models. Refinements under these space groups *I*2/*m* and *Im* have been also performed but worse R-factor values were obtained. In particular, refinement with *I*2/*m* symmetry converge to an R = 5.2%, whereas refinement in *Im* gives a similar R-factor but high correlations between parameters. For these reason the monoclinic models were discarded and only the orthorhombic model was considered for further discussion and comparison with the modulated models.

4. Results and Discussion

4.1. Structures of $LiCdVO_4$ ($x = 0$) and $Li_{7/9}Cd_{1/9}\square_{1/9}CdVO_4$ ($x = 1/3$). The crystal structure of $LiCdVO_4$ and $Li_{7/9}Cd_{1/9}\square_{1/9}CdVO_4$ is illustrated in Figure 7A and mainly characterized by edge-sharing [$Cd1O_6$] octahedra chains. These chains are isolated from each other and parallel to the **c** axis (Figure 7B). These chains are linked together by [$V1O_4$] and [(Cd2/Li2/□)O_4] tetrahedra by sharing corners. The [$V1O_4$] and [(Cd2/Li2/□)O_4] tetrahedra share both an edge (O1−O1) parallel to the **a** axis and corners (O2) along the **c** axis, resulting in double chains that run parallel to the **c** axis (Figure 7b). The [$Cd1O_6$] octahedron is almost regular with average Cd1−O distance equal to 2.288 and 2.289 Å for $LiCdVO_4$ and $Li_{7/9}Cd_{1/9}\square_{1/9}CdVO_4$, respectively. These distances are in good agreement with the value calculated from Shannon table, 2.33 Å.[15] The bond valence sums (BVS) calculated are equal to 2.13 and 2.12 for Cd1 position in $LiCdVO_4$ and $Li_{7/9}Cd_{1/9}\square_{1/9}CdVO_4$, respectively, and in good agreement with the expected value +2 (the bond valence parameters are taken from ref 16, see Table 4). In the double chain of [$V1O_4$] and [(Cd2/Li2/□)O_4] tetrahedra steric strains appear and induce a distortion of the coordination polyhedra.

(15) Shannon, R. D. *Acta Crystallogr., Sect. A: Found. Crystallogr.* **1976**, *32*, 751.
(16) Brese, N. E.; O'Keefe, M. *Acta Crystallogr., Sect. B: Struct. Sci.* **1991**, *47*, 192.

Table 7. Final Atomic Coordinates, Fourier Amplitudes of the Occupancy and Displacive Modulation Functions, and Equivalent Isotropic Thermal Displacements of Compounds with Composition $x = 3/4$ for Section $t = 1/16$, *Im2m* Space Group[a]

atom		occ.	*x*	*y*	*z*	U_{eq}
Cd1			0	0	0.5	0.01203(10)
	s,1		0	0.01030(5)	0.00239(8)	
	c,1		0	0	0	
	s,2		0	0.00379(13)	0.00273(19)	
	c,2		0	0	0	
	s,3		0	0.0017(3)	0.0020(4)	
	c,3		0	0	0	
Cd2		0.25	0	0.316(2)	0.75	0.040(3)
	s,1	0	0	0	0.009(2)	
	c,1	0.277(2)	0	−0.020(3)	0	
	s,2	0	0	0	−0.0045(18)	
	c,2	0.045(3)	0	0.0091(17)	0	
Li2		0.5	0	0.325	0.75	0.017(5)
	s,1	0	0	0	−0.022(10)	
	c,1	−0.5	0	0.027(3)	0	
V1			0	0.64206(7)	0.75	0.0104(2)
	s,1		0	0	−0.0010(2)	
	c,1		0	−0.00128(13)	0	
	s,2		0	0	−0.0065(3)	
	c,2		0	−0.0003(2)	0	
	s,3		0	0	0.0019(10)	
	c,3		0	0.0000(6)	0	
O1			0.2615(4)	0.0261(2)	0.75	0.0136(5)
	s,1		0	0	0.0000(4)	
	c,1		−0.0045(4)	0.0093(3)	0	
	s,2		0	0	−0.0021(7)	
	c,2		0.0010(13)	−0.0003(6)	0	
O2			0	0.2512(3)	0.4538(4)	0.0241(7)
	s,1		0	0.0045(3)	−0.0021(5)	
	c,1		0	0.0014(3)	0.0021(5)	
	s,2		0	0.0011(6)	−0.0004(9)	
	c,2		0	0.0037(6)	0.0105(9)	

[a] Occupancy modulation is $P = P_o + c_1\cos(2\pi x_4) + c_2\cos(4\pi x_4)$ Displacive modulation is $U = s_n(\sin(2\pi n x_4) + c_n\cos(2\pi n x_4)$.

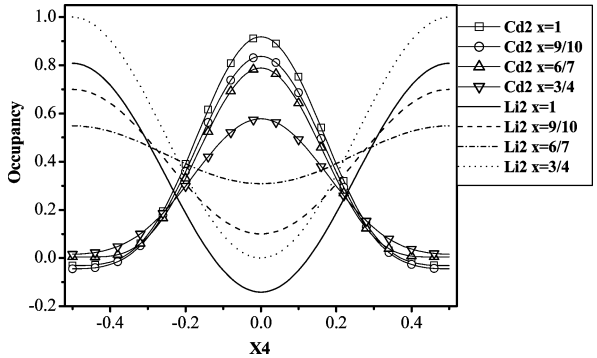

Figure 6. Cd2 and Li2 occupancy modulations of compounds $x = 1$, $9/10$, $6/7$, and $3/4$.

Table 8. Crenel Parameters of Cd2 Atom and Convergence R-Factors[a]

	$x = 1$	$x = 9/10$	$x = 6/7$	$x = 3/4$
x/3	0.3333	0.3000	0.2857	0.250
Δ	0.4329(9)	0.4261(9)	0.441(1)	0.503(1)
p	0.762(4)	0.713(4)	0.624(4)	0.480(2)
R	3.23	3.57	4.13	4.00
R_0	2.23	1.92	3.06	2.41
R_1	4.16	3.13	4.05	7.09
R_2	7.42	13.23	8.41	18.78

[a] *x*/3 is the fully occupied expected crenel-width derived from the composition, Δ and *p* are the refined crenel-width and the fractional occupancy of the crenel. R_0, R_1, R_2 are the reliability factors for the main and satellite reflections of first and second order, respectively.

As said before, the $[V1O_4]$ and $[(Cd2/Li2/\square)O_4]$ tetrahedra share an edge (O1−O1) that induces a short V1−Li2 distance equal to 2.67(3) and 2.717(9) Å for $LiCdVO_4$ and $Li_{7/9}Cd_{1/9}\square_{1/9}CdVO_4$, respectively. A shift of these cations away from the center of the tetrahedra to maximize these distances is observed with V1−O1 and Li2−O1 distances longer than V1−O2 and Li2−O2 distances, see Table 4 and Figure 7b. These results are confirmed by the bond-valence calculation. The calculated values of 5.12 and 5.09 for

Table 9. Atomic Parameters of Compound with Composition $x = 3/4$ in the Three-Dimensional Supercell and Space Group *Im2m*

atom	occ.	*x*	*y*	*z*	U_{eq}
Cd11	1	0	0.0039(4)	0.06244(7)	0.0041(5)
Cd12	1	0	0	0.81340(10)	0.0160(5)
Cd13	1	0	0.9920(5)	0.31245(12)	0.0235(5)
Cd14	1	0	0.9871(3)	0.56155(7)	0.0103(6)
V1	1	0	0.6413(9)	0.87562(20)	0.0162(16)
V2	1	0	0.3605(8)	0.7491(2)	0.0135(15)
V3	1	0	0.6368(8)	0.37645(17)	0.0085(12)
V4	1	0	0.3481(8)	0.5	0.0033(14)
V5	1	0	0.3491(10)	0	0.017(2)
Cd21	0.502(2)	0	0.6860(9)	0	0.025(2)
Cd22	0.464(9)	0	0.2949(8)	0.37359(15)	0.0161(13)
Cd23	0.286(4)	0	0.6871(9)	0.7513(2)	0.026(2)
Li3	0.5	0	0.728(8)	0.757(3)	0.018317
Li4	1	0	0.321(3)	0.8652(10)	0.000454
Li5	1	0	0.629(5)	0.5	0.018552
O11	1	0.249(3)	0.0320(14)	0.3743(3)	0.015(3)
O12	1	0.5	0.2483(16)	0.3253(6)	0.018(4)
O13	1	0.5	0.2397(16)	0.5752(8)	0.046(6)
O21	1	0.231(2)	0.4696(15)	−0.2507(4)	0.015(3)
O22	1	0	0.2643(16)	−0.1929(5)	0.011(4)
O23	1	0	0.2576(14)	0.3085(4)	0.015(3)
O31	1	0.260(2)	0.0131(14)	0.1240(3)	0.012(3)
O32	1	0.5	0.243(2)	0.0819(8)	0.048(6)
O33	1	0	−0.2483(17)	0.3297(4)	0.020(3)
O41	1	0.233(4)	0.4648(18)	0.5	0.017(5)
O42	1	0	0.2236(17)	0.5473(5)	0.010(4)
O52	1	0	0.2450(15)	0.0541(6)	0.021(4)
O51	1	0.230(3)	0.475(2)	0	0.013(5)

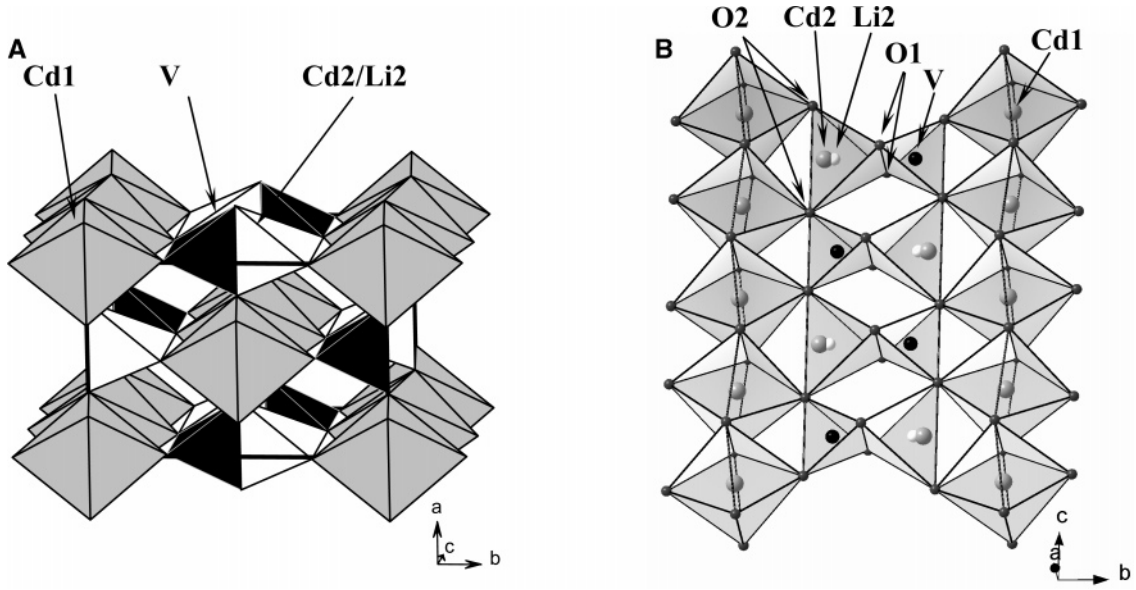

Figure 7. Octahedral packing view of the $Li_{1-2x/3}Cd_{x/3}CdVO_4$ structures along the (A) **c**-direction and (B) **a**-direction.

vanadium and 0.81 and 0.73 for lithium in $LiCdVO_4$ and $Li_{7/9}Cd_{1/9}\square_{1/9}CdVO_4$, respectively, are in good agreement with the expected values of +5 and +1. The cadmium atoms replace lithium atoms in the [$Li2O_4$] tetrahedral site in a different crystallographic site. Indeed, a shift in **b** direction is observed away from sharing O1−O1 edge of the [$V1O_4$] tetrahedra, to increase cation−cation distance with vanadium (Table 4). The cation−cation distance increase is correlated to the cationic radii size difference between Li^+ (0.59 Å for coordination number CN = 4) and Cd^{2+} (0.78 Å, CN = 4).[15] In $Li_{7/9}Cd_{1/9}\square_{1/9}CdVO_4$ the shift of the cadmium position away from the O1−O1 edge through the O2−O2 edge induces a short Cd2−O2 distance, 1.9536(15) Å. These internal strains can be correlated with the high atomic displacement parameters U_{33} (0.03 $Å^2$) of the O2 atomic position. This oxygen motion or disorder tends to increase the distance between Cd2 and O2. A refinement model with split O2 positions has been tested but if two positions were indeed refined their occupancy ratios were not satisfactory. Use of a unique position for O2 atoms led to 2 short Cd2−O2 distances and explains the relatively high value of the Cd2 BVS, 2.38. When the amount of cadmium in the [(Cd2/Li2/□)O_4] tetrahedra increases, the steric strains also increase and a rearrangement of the structure is necessary which can be associated with the observation of the modulation of the structure. These steric strains prevent to exceed the limit composition $Li_{1/3}Cd_{1/3}CdVO_4$ ($x = 1$). Indeed, from a chemical point of view the limit composition would be $Cd_{1/2}CdVO_4$ where the lithium atom in the tetrahedral site is replaced by one-half of cadmium. However, attempts to synthesize compounds with x value higher than 1 have failed.

4.2. Structures of $Li_{1/2}Cd_{1/4}CdVO_4$ ($x = 3/4$), $Li_{3/7}Cd_{2/7}CdVO_4$ ($x = 6/7$), $Li_{4/10}Cd_{3/10}CdVO_4$ ($x = 9/10$), $Li_{1/3}Cd_{1/3}CdVO_4$ ($x = 1$). The structural modulation and the variation of the wavevector are associated with the distribution of the $(1 - 2x/3)Li/(x/3)Cd$ atoms on one single site (0, 0.30, 0.75) of the basic structure. Such a distribution has been modeled first with two anti-phase modulations $P(x_4)$, which concentrate the occupancies of Cd2 and Li2 around the values $x_4 = 0$ and 0.5, respectively (see Figure 6). This figure sketches the function

$$P(x_4) = P_o + P_1\cos(2\pi x_4) + P_2\cos(4\pi x_4)$$

with P_o, P_1, and P_2 being the occupancy coefficients given in Tables 5−7. The maximal amplitude of the occupancy of Cd2 decreases from a maximum close to 1 for the compound $x = 1$ to 0.6 for $x = 3/4$. From these functions, it is easy to follow throughout the **c**-direction of the crystal the Cd2/Li2 concentration for a given position. A unit cell jump along the **c**-axis from a Cd2-position in an arbitrary basic cell associated with a specific x_4 value leads to an equivalent atom whose occupancy value is given by the modulation function $P(x_4)$ at an x_4 value shifted an amount γ from the previous one. On the other hand, symmetry equivalent positions in the basic unit cell have associated symmetry related occupancy functions, giving an identical or 1/2-shifted function depending on the symmetry operation. As an example, for the composition $x = 3/4$, the Cd2/Li2 occupancy of four symmetry related positions in a basic unit cell are given in Table 10. It can be seen from this result that Cd2 and Li2 occupy each position with a different probability along the crystal. Consecutive c-translated positions have associated successive γ-shifts along the internal coordinate x_4 and, for an irrational γ-value value, all values of the occupancy functions occur when an infinite number of unit cells are considered. However, if γ has a rational value, like in the case of composition $x = 3/4$, the successive γ -shifts mean that only four different x_4 values are obtained and the harmonic functions are only evaluated at four different values. In this case, the sums of Cd2 and Li2 occupancies in any cell are 1 and 2, respectively, and they are constant along the crystal, but the distribution over four symmetry related positions changes from cell to cell with γ -shifts in the occupancy functions. Note that the result does not keep for any other phase with a different γ-value, where the sum of occupancies associated with four symmetry related Cd2 atoms in a basic cell is given by $4P_o + 4P_2\cos(4\pi x_4)$.

Table 10. Cd2/Li2-Occupancy on the Four Symmetry-Related Position in a Basic Unit Cell for $x = {}^3/_4$[a]

	coordinates	occupancy F($S_n^{-1}x_4$)	
symmetry	(x, y, z)	Cd2	Li2
$S_1(x, y, z, x_4)$	(0, 0.316, 0.75)	0.026	0.962
$S_2(x, -y, {}^1/_2 + z, x_4)$	(0, 0.684, 0.25)	0.324	0.309
$S_3({}^1/_2 + x, {}^1/_2 + y, z, {}^1/_2 + x_4)$	(1/2, 0.816, 0.75)	0.538	0.038
$S_4({}^1/_2 + x, {}^1/_2 - y, {}^1/_2 + z, {}^1/_2 - x_4)$	(1/2, 0.184, 0.25)	0.112	0.691

[a] The special positions reduce to four the number of relevant symmetry operations. Coordinates give the four symmetry related sites in the unit cell. The occupancy is calculated using the coefficients given in Table 7 with $x_4 = qz$. Note that the total occupancy in the unit cell is 1 for Cd2 and 2 for Li2, corresponding to the formula composition.

The refinements of the occupancies with crenels instead of continuous functions show an unexpected result. The key parameter of this refinement sumarized in Table 8 is the crenel-width. A fully ordered model based on crenel functions would correspond to crenel-widths fixed by the composition (x/3 for Cd2) and full occupation of the position. In this case, positions with associated x_4 coordinate inside the crenel would be fully occupied, whereas outside the crenel they are vacant. However, as commented previously, the best refinement results were obtained when the crenel-width and occupancy parameters were refined variables, obtaining the values of Table 8. All the crenel-width values are larger than the x/3 value and, consequently, the crenels are partially occupied.

A partially occupied Cd2-crenel allows this atom to share position with the Li2 in an ordered or disordered manner, which could not be discriminated from either the continuous or the crenel refinements. Nevertheless, this is an aspect that could be clarified by looking at the structural result of the standard three-dimensional analysis of the $x = {}^3/_4$ phase. Also, a comparison with the four-dimensional description is a good test of the validity and proximity of the superspace model against the three-dimensional one.

The superspace continuous model approach for $x = {}^3/_4$ and the commensurate character of the wavevector are both gathered in the x_4-x_3 plot of Figure 8, where Cd2 atoms are represented by atomic domains covering an x_4-extension where the occupancy is greater than 0.05 (the rest of the atomic domains are omitted for simplicity). The independent atomic domain Cd2 referenced in Table 7 is that centered at $x_3 = 0.75$, $x_4 = 0$ (named A), with an associated occupancy modulation function defined by the coefficients given in Table 7 and represented in Figure 9 together with Li2. Owing to the special position of Cd2, only four different domains are generated by the superspace group symmetry with center coordinates Cd2-A(0, y, ${}^3/_4$, 0), Cd2−B(0, $-y$, ${}^1/_4$, 0), Cd2−C(${}^1/_2$, ${}^1/_2 + y$, ${}^3/_4$, ${}^1/_2$) and Cd2-D(${}^1/_2$, ${}^1/_2 + y$, ${}^1/_4$, ${}^1/_2$). Figure 8 also includes the commensurate points realized in the *Im*2*m* 3D-structure, i.e., the Cd2-A atomic domains at points $x_3 = {}^3/_4$ and $x_4 = {}^1/_8$, ${}^3/_8$, ${}^5/_8$, and ${}^7/_8$. These points are the only relevant ones in the commensurate structure and have occupancy values 0.446, 0.054, 0.054, and 0.446 respectively, as derived from the function $P(x_4)$ of Table 7. In the symmetry related domain Cd−B(0, $-y$, ${}^1/_4$, x_4), cuts are at $x_4 = 0$, ${}^1/_4$, ${}^1/_2$, and ${}^3/_4$ and the occupancy function values are 0.572, 0.205, 0.018, and 0.205, respectively. This set of values represents the Cd2-occupancies taking place in the crystal, which should be, in principle, coincident with those determined in the three-dimensional refinement. This result from the superspace approach is gathered in Figure 9, where

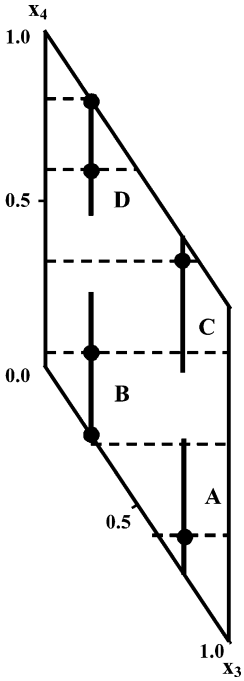

Figure 8. $x3-x4$ Projection of the crenel-model superspace unit cell for compound $x = {}^3/_4$. The Cd2-atomic domains are extended to cover an $x4$-region where $P(x4) > 0.05$. Dashed lines mark the commensurate sections giving a 3D structure with *Im*2*m* symmetry. Black filled circles represent Cd2 positions and open circles are inversion centers of the superspace group.

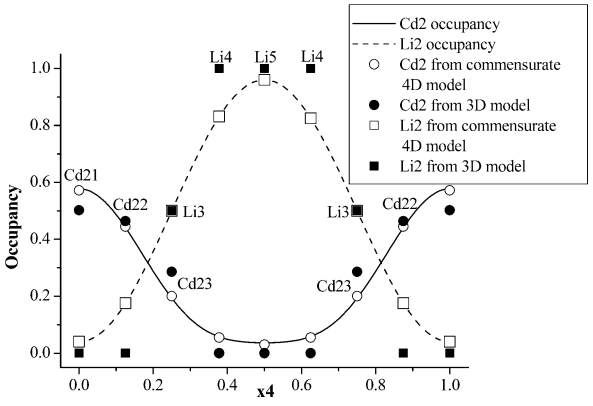

Figure 9. Plot of the occupancy functions of Cd2 and Li2 of the $x = {}^3/_4$ superspace model. Open symbols on the curves (circle and square) represent the values which are realized in the corresponding 3D structure. The filled symbols correspond to the values of the supercell model refined with standard methods.

the continuous functions of the superspace model are represented together with the relevant points realized in the structure. We can now compare this result with the three-dimensional structural model of the compound $x = {}^3/_4$ refined by standard methods. Using the parameters of Table 8, the supercell $4c_o$ drawn in Figure 10 contains 4 basic subcells and the atomic sites are occupied with different fractions of

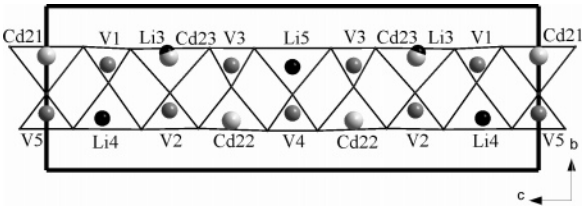

Figure 10. *bc* Projection of the $x = {}^3/_4$ structure described in the *Im*2*m* three-dimensional supercell. For simplicity, only Cd2/Li2 and vanadium tetrahedral sites located at $x \approx 0$ are represented.

Table 11. Comparison of the Cd2/Li2 Occupancy Distributions between the Four-Dimensional and Three-Dimensional Models for Compound $x = {}^3/_4$[a]

			Cd2		Li2	
crenel	atom	x_4	$P(x_4)$	P(Cd2)	$P(x_4)$	P(Li2)
A	Cd22	0.125	0.446	0.464	0.146	0
	Li4	0.375	0.054	0	0.854	1
	Li4	0.625	0.054	0	0.854	1
	Cd22	0.875	0.446	0.464	0.146	0
B	Cd21	0	0.572	0.502	0.000	0
	Cd23/Li3	0.25	0.205	0.286	0.500	0.5
	Li5	0.5	0.018	0	1.000	1
	Cd23/Li3	0.75	0.205	0.286	0.500	0.5

[a] $P(x_4)$ is the harmonic function and P(Cd2)/P(Li2) are the occupancies refined in the 3D model.

Cd2/Li2 atoms as resulted from the refined structure (Table 8). Note that atoms are ${}^1/_4\mathbf{c}$ ($= \mathbf{c_o}$) or ${}^1/_8\mathbf{c}$ ($= {}^1/_2\mathbf{c_o}$) away from each other and the *z*-coordinate is the only relevant parameter to establish the relationship between the four- and three-dimensional descriptions. To compare the spatial distribution of atoms along the **c**-direction in Figure 10 with the atomic sequence along x_4 in Figure 9, a real space translation $\Delta\mathbf{c}$ corresponds to a phase shift $q\Delta\mathbf{c}$ in x_4. Using the occupancy function of Cd2 and starting with the Cd21 atom (P(Cd21) = 0.502) in Figure 10, the equivalent point in the superpace model is Cd21 at $x_4 = 0$ in Figure 9. A translation of the basic vector $\mathbf{c_o}$ leads to a shared position occupied by Cd23 (P(Cd23) = 0.286), whereas in the superspace diagram a phase shift of $q\mathbf{c_o} = 0.75$ has to be applied leading to the Cd23 position at $x_4 = 0.75$ and $P(0.75) = 0.2$. An additional translation $\mathbf{c_o}$ falls into the labeled Li5 atom (empty of Cd2) and the corresponding x_4 coordinate shifts to 0.5 with a $P(0.5) = 0$. By repeating this procedure all the Cd2-atoms are run and the corresponding points in Figure 9 are found. All these results are summarized in Table 11 where some discrepancies between the two models are evidenced. The reason for these differences is the assumed simplicity in the 3D model where Cd2 atoms were placed only on three positions, whereas the continuous occupancy four-dimensional model gives a distribution $P(x_4)$ for Cd2 atoms concentrated on the same three positions and small amounts on three additional positions. Taking into account these residual positions in the 3D model, with fixed occupancies as derived from the $P(x_4)$ function, does not improve the R-factor index or the above-mentioned discrepancies.

As previously described in the structural study of $LiCdVO_4$ and $Li_{7/9}Cd_{1/9}CdVO_4$ (previous section) and $Li_{1/3}Cd_{1/3}CdVO_4$ [8] a *y*-coordinate change is observed between Li2 and Cd2 atoms. Owing to the AMF, the interatomic distances vary along the crystal as shown in Table 12. The behavior of the distances along the internal coordinate *t* is similar to that

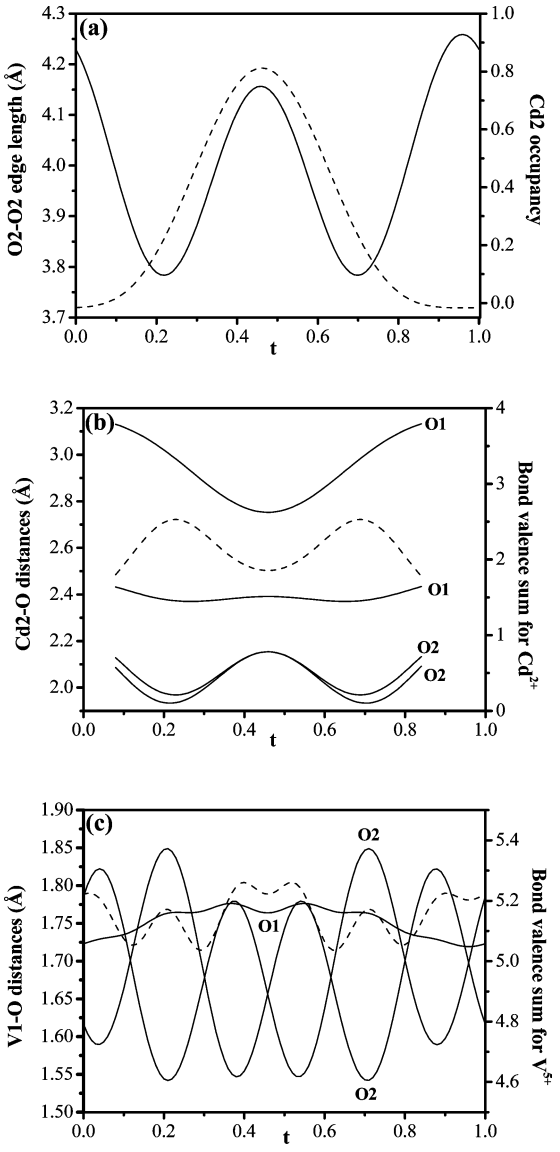

Figure 11. Interatomic distances and bond valence (dashed lines) variations versus internal phase parameter *t* in the $Li_{0.4}Cd_{0.3}\square_{0.3}CdVO_4$ ($x = {}^9/_{10}$) crystal structure: (a) variation of the O2−O2 edge length of the [(Li2/Cd2/□)O_4] tetrahedral; the dashed line is the occupancy modulation of Cd2; (b) variation of the Cd2−O and bond valence sum of Cd2; and (c) variation of V1−O distances and the bond valence sum V1.

described by Gaudin et al.[8] for the compound $x = 1$ so that arguments given there can be extrapolated here. As previously mentioned in the discussion section about $LiCdVO_4$ and $Li_{7/9}Cd_{1/9}CdVO_4$ structures, the shift of Cd2 position away from the disordered [Li2/Cd2/□] tetrahedra, to increase V1−Cd2 distance, induces steric strains. The Cd2 atoms getting closer to the O2−O2 edge makes the Cd2−O2 distance become too small and an elongation of the O2−O2 edge is expected to increase the Cd2−O2 distances. In Figure 11a−c the O2−O2, Cd2−O, and V1−O distances for the composition $x = {}^9/_{10}$ are given; these results are close to the ones observed for the other modulated compounds. In Figure 11a the *t* domain where the $P(x_4)$ occupancy modulation function has a significant occupancy of the tetrahedra by Cd2 atoms corresponds to an O2−O2 distance increase. This induces an increasing of the Cd2−O2 distances in the same *t* domain as shown in Figure 11b and the bond-valence sum is reduced close to +2 around the maximum of occupancy

Table 12. Selected Interatomic Distances

	$x = 9/10$			$x = 6/7$			$x = 3/4$		
	av	min	max	av	min	max	av	min	max
Cd1−O1	2.295(8)	2.206(12)	2.401(10)	2.295(2)	2.263(2)	2.339(2)	2.290(5)	2.277(5)	2.305(6)
Cd1−O2	2.285(12)	2.178(14)	2.39(2)	2.294(5)	2.227(4)	2.358(5)	2.290(9)	2.231(9)	2.343(9)
Cd2−O1	2.387(7)	2.370(6)	2.434(6)	2.394(4)	2.376(3)	2.440(3)	2.361(19)	2.318(19)	2.403(19)
Cd2−O2	2.038(7)	1.933(7)	2.154(8)	2.034(5)	1.931(5)	2.163(5)	2.07(2)	2.01(2)	2.19(2)
Li2−O1	2.34(7)	2.30(7)	2.40(6)	2.22(2)	2.08(2)	2.42(2)	2.299(13)	2.102(12)	2.496(13)
Li2−O2	2.10(3)	1.96(3)	2.26(3)	2.150(12)	1.979(14)	2.302(12)	2.11(3)	1.97(3)	2.29(3)
V1−O1	1.753(11)	1.72(2)	1.776(4)	1.754(5)	1.727(8)	1.779(2)	1.749(3)	1.734(3)	1.765(3)
V1−O2	1.688(14)	1.542(11)	1.849(11)	1.677(7)	1.535(5)	1.835(5)	1.674(7)	1.642(7)	1.709(7)

for Cd2 atoms at around $t = 0.45$ (or $x_4 = 0$). The increasing O2−O2 distance is also observed in the t domain where the tetrahedral site is occupied by lithium (around $t = 0$). The smallest O2−O2 distance is observed when the tetrahedral site is empty. This large variation of the O2−O2 distance induces a strong perturbation for the corner-sharing [$V1O_4$] tetrahedra (Figure 7b) and explains the strong V1−O2 distances variations (Figure 11c). Nevertheless, the bond-valence sum of vanadium atoms oscillates weakly around the value of +5.1, which is close to the expected value (Figure 11c).

From the present study it seems clear that the driving mechanism of the structural modulation in these compounds can be considered the general tendency of the Li atoms in the Li2 sites to be as far apart as possible (once a nonhomogeneous occupation of the sites becomes necessary because of the steric strains mentioned above). This is seen in the superspace representation of the structures (see, for instance, Figure 8) by the fact that the occupational modulations of neighboring Cd2/Li2 sites are such that in general Cd and Li predominant intervals alternate along x_4, and the intervals which are mainly Li-occupied are close together when projected on the x_4 axis, but they do not superpose. We can call this approximate topological feature of the Li2 occupational modulation a kind of "*weak closeness condition*". This is reminiscent of the situation occurring in many families of compounds and homologous series with flexible composition, where minority motifs or atoms are distributed uniformly along some direction so that they constitute a modulated structure. The superspace description of these compounds requires steplike occupational modulations in the form of crenel functions, and a so-called exact *closeness* condition of these crenel functions is fulfilled (i.e., when projected on the x_4 axis, the crenel functions associated with consecutive sites are close together but without superposition, i.e., the two projected intervals touch). This strict mathematical condition on the occupational modulation forces, in general, a specific relation between composition and modulation wave vector which can be predicted and used as a chemical ruler.[17,18] Furthermore a unique superspace group symmetry is usually valid for all compositions. In the case of the $Li_{1-2x/3}Cd_{x/3}\square_{x/3}CdVO_4$ system, something similar is happening, and a unique superspace group is valid for all compositions with modulated configurations, while the modulation wave vector varies linearly with composition. However, a local ordering of the Li, Cd, and vacancies is not fully realized, and the actual occupational modulations seem better-described by continuous functions rather than crenel functions. An exact closeness condition of different atomic occupational domains is then not possible, as Cd and Li atoms share a good proportion of the sites along the modulation, and no definite border between Cd and Li domains can be defined. But the continuous modulations keep, however, a kind of *weak closeness condition*, in the sense mentioned above. This condition explains the general tendency of the modulation wave vector to decrease as x increases, as a consequence of the corresponding decrease of the effective Li-dominant interval along its modulation function. It is clear, however, that a predictable correlation between the Li content and the modulation wave vector cannot be derived from the model. One can only expect a much weaker variation of the wave vector with composition, as it is in fact the case.

5. Conclusion

In the system $(1 - x)LiCdVO_4 - xLi_{1/3}Cd_{1/3}\square_{1/3}CdVO_4$ the replacement of lithium by cadmium in the disordered tetrahedral site induces strong steric strains. When cadmium content is high, with x value greater than or equal to 0.75, modulated structures have been observed and can be associated with the adaptation of the structure to the steric strains. These steric strains are caused by the shift of the cadmium position away from the tetrahedral center to increase the cation−cation distance between V^{5+} and Cd^{2+}, leading to Cd−O distances that are too short. These steric strains are so strong that synthesis of compounds with x value higher than 1 were unsuccessful. The compound $Cd_3(VO_4)_2$, which can be rewritten $Cd_{1/2}\square_{1/2}CdVO_4$, corresponds to the replacement of all lithium by $^1/_2$ of cadmium. It crystallizes with a different structure. This result is in agreement with our study since the $LiCdVO_4$ (Na_2CrO_4-type) structure is not flexible enough to manage a realistic distance for such a large amount of cadmium. Work is in progress to study the crystal structure of $Cd_3(VO_4)_2$, which is not known.

Acknowledgment. We acknowledge the assistance of E. Castel for powder sample preparation. F.J.Z. and J.M.P.-M. acknowledge financial support of this work by the Spanish MCYT Project BFM2002-00057.

Supporting Information Available: Tables of anisotropic displacement parameters, tables of final displacement parameters and SDP modulation functions (pdf), and crystallographic information files (cif). This material is available free of charge via the Internet at http://pubs.acs.org.

CM050104E

(17) Perez-Mato, J. M.; Zakhour-Nakhl, M.; Weil, F.; Darriet, J. J. *Mater. Chem.* **1999**, *9*, 2795.
(18) Elcoro, L.; Prez-Mato, J. M.; Withers, R. *Z. Kristallogr.* **2000**, *215*, 727.